nature communications

Article

https://doi.org/10.1038/s41467-025-58184-9

On-demand treatment of metabolic diseases by a synthetic drug-inducible exocytosis system

Received: 31 March 2024

Accepted: 14 March 2025

Published online: 22 March 2025

Check for updates

Yaqing Si[1,2,3,4,5,11], Minghui He[1,2,3,4,5,11], Yilin Li[2,3,4,5,6,11], Jian Jiang[2,3,4,5,7], Yuxuan Fan[2,3,4,5,6], Shuai Xue[2], Xinyuan Qiu[8,9] & Mingqi Xie[2,3,4,5,10]

Here, we present StimExo as a rational design strategy allowing various user-defined control signals to trigger calcium-dependent exocytosis and mediate on-demand protein secretion in cell-therapy settings. Using a modular framework incorporating inducible protein-protein interactions into an engineered bipartite activator of calcium release–activated calcium (CRAC) channels, Ca^{2+} influx mediated by the STIM/Orai1 machinery was flexibly adjusted to depend on different user-defined input signals. Application of StimExo to various endocrine cells enables instant secretion of therapeutic hormones upon administration of safe and patient-compliant trigger compounds. StimExo also mediated insulin exocytosis using a cell-based gene delivery strategy in vivo, accounting for real-time control of blood glucose homeostasis in male diabetic mice in response to the FDA-approved drug grazoprevir. This study achieves true "sense-and-respond" cell-based therapies and provides a platform for remote control of in vivo transgene activities using various trigger signals of interest.

Cell-based therapy, which involves administration of cells as living agents to fight diseases, is experiencing explosive growth owing to its unique capability to custom-design smart therapeutic algorithms within patients[1]. For example, human cells can be programmed with sophisticated sense-and-response functions by synchronizing expression of the therapeutic transgene(s) with endogenous disease metabolite levels or external trigger signals[1,2]. However, most transgene regulation strategies used in such advanced therapy medicinal products (ATMPs) are based on transcriptional control, which have relatively slow response rates[3]. Though transcription-based cell therapies are sufficient to treat many chronic diseases such as obesity[4], liver failure[5], insulin resistance[6], type-2 diabetes[7], or cancer[8], faster gene regulation strategies are urgently required for treatments that necessitate on-demand secretion of therapeutic proteins within minutes.

Synthetic biology is an engineering-driven discipline that keeps establishing powerful gene regulation tools to enhance the safety, efficacy and clinical eligibility of modern gene and cell-based therapies[9,10]. In recent years, many post-transcriptional regulation schemes have been described with the goal to improve protein secretion rates. While translational regulation is indeed significantly faster than conventional transcription[11], there is still a typical delay of two hours in time between the moments of stimulation and noticeable protein production[12]. For treatment of acute conditions such as type-1 diabetes, chronic pain or cardiovascular diseases, the kinetics of

[1]School of Basic Medical Sciences, Fudan University, Shanghai, China. [2]Westlake Laboratory of Life Sciences and Biomedicine, Hangzhou, Zhejiang, China. [3]Key Laboratory of Growth Regulation and Translational Research of Zhejiang Province, School of Life Sciences, Westlake University, Hangzhou, Zhejiang, China. [4]Institute of Basic Medical Sciences, Westlake Institute for Advanced Study, Hangzhou, Zhejiang, China. [5]School of Medicine, Westlake University, Hangzhou, Zhejiang, China. [6]College of Life Sciences, Zhejiang University, Hangzhou, Zhejiang, China. [7]School of Life Sciences, Fudan University, Shanghai, China. [8]Department of Biology and Chemistry, College of Science, National University of Defense Technology, Changsha, Hunan, China. [9]College of Computer Science and Technology, National University of Defense Technology, Changsha, Hunan, China. [10]School of Engineering, Westlake University, Hangzhou, Zhejiang, China. [11]These authors contributed equally: Yaqing Si, Minghui He, Yilin Li. e-mail: xiemingqi@westlake.edu.cn

translational regulation strategies are therefore still insufficient. Faster timescales (30-60 min) were achieved in a multitude of approaches that capitalize on introduction of programmable proteases into the secretory pathway of mammalian cells[13–15], but only regulation mechanisms involving vesicular exocytosis may qualify as on-demand protein secretion in its strictest sense[16,17]. So far, trigger-inducible exocytosis was only achieved through ectopic expression of naturally evolved temperature[18]-, voltage[19]- or light-sensitive ion channels into secretory cell types[20]. A rational and universal approach on the contrary, which would enable any user-defined trigger signal to regulate target protein exocytosis in clinically eligible cell therapy contexts, is still elusive.

Here, we describe StimExo as a framework to engineer trigger-inducible bipartite STIM1 effectors, whose active conformation is exclusively formed through pre-programmed protein-protein interactions (PPIs). Stromal interaction molecule (STIM1) is an integral component of calcium release activated Ca^{2+} (CRAC) channels naturally residing in the ER membrane as a dimer. Depletion of Ca^{2+} in the ER induces rapid formation of STIM1 oligomers capable of translocating to the plasma membrane and activating the pore-forming channel subunit Orai1[21,22]. In StimExo, the luminal Ca^{2+}-binding domain of native STIM1 was replaced by various synthetic oligomeric proteins and co-expressed as a separate polypeptide alongside the cytoplasmic Orai1-interacting STIM1ct domain. Both moieties were then fused to different conditional PPI pairs, rendering reconstitution of a full CRAC effector exclusively dependent on trigger-inducible protein dimerization. In this manner, calcium influx into diverse mammalian cell types could be effectively governed by different types of small molecule triggers, such as the FDA-approved drugs grazoprevir or rapamycin analogues. Using StimExo, trigger-inducible exocytosis of various therapeutic payloads from various human endocrine cell types was achieved within a few minutes after stimulation. To exemplify therapeutic efficacy in a cell therapy setting, pancreatic host cells stably transgenic for StimExo and proinsulin expression were encapsulated into alginate-poly-L-lysine-alginate beads and implanted into type-1 diabetic mice, ultimately resulting in real-time control of blood glucose levels upon grazoprevir administration. Taken together, StimExo not only helps overcoming a critical hurdle that was hitherto prohibiting instant and customizable “sense-and-respond” cell-based therapies, but can also be generally applied to manipulate a wide range of calcium-dependent physiological processes in either basic research or applied life sciences.

Results

Synthetic CRAC activators based on spontaneous STIMct oligomerization

Calcium (Ca^{2+}) release activated Ca^{2+} (CRAC) channels are involved in a variety of signaling pathways of human cells, including exocytosis, gene expression, energy homeostasis and apoptosis[22,23]. CRAC channels are ubiquitously expressed in many cell types, typically comprising an intracellular stromal interaction molecule (STIM1) protein and a pore forming Orai1 subunit located in the plasma membrane[22]. In its natural context, STIM1 acts as a Ca^{2+} sensor bridging the endoplasmic reticulum (ER) and the plasma membrane to mediate intracellular calcium homeostasis[24,25]. Under resting conditions, STIM1 resides in the ER as a dimer, but once ER luminal calcium is depleted, the Ca^{2+}-binding canonical EF-hand domain of STIM1 will undergo a rapid conformational change, leading to unfolding of coiled-coil (CC) domains and cytoplasmic exposure of the STIM-Orai activating region (SOAR), which triggers the formation of an oligomerization state that allows STIM1 to translocate to plasma membrane and activate Orai1 within few seconds[21] (Fig. 1A). To engineer a universal trigger-inducible CRAC activator coupling other input signals of interest to regulation of Orai1-mediated calcium influx, we replaced the Ca^{2+}-sensitive ER-luminal domain of native STIM1 by a synthetic oligomeric protein. Thus, Orai1-activation efficiency will exclusively depend on the oligomerization status of the polypeptide that contains a cytoplasmic STIM1ct domain; while fusion of a monomeric protein to STIM1ct is expected to yield a resting STIM1ct molecule incapable of membrane translocation and Orai1-activation, fusion of higher-order oligomers to STIM1ct would spontaneously form an aggregated STIM1ct complex that resembles the oligomeric state that was naturally triggered through EF-domain-mediated CC/SOAR unfolding (Fig. 1A). To test this hypothesis, we first fused different fluorescent proteins of similar molecular weight but differing in their native oligomerization states (Fig. 1B). According to literature reports[26], mCherry and mRuby3 are monomeric proteins, whereas enhanced green fluorescent protein (EGFP) and Azami-Green (AG) form dimers and tetramers in mammalian cells, respectively. Indeed, native PAGE experiments confirmed that 3xFLAG-tagged mCherry-STIM1ct, mRuby3-STIMct and EGFP-STIM1ct all show a band indicating the formation of putative dimers or monomers, but in the lane of 3xFLAG-AG-STIM1ct, this band was not detected, and its blotted position was much higher, which is indicative for higher-order oligomeric states (Fig. 1B). Using confocal microscopy, we further show that tetrameric 3xFLAG-AG-STIM1ct had highest membrane translocation efficiency, while monomeric 3xFLAG-mCherry-STIM1ct and 3xFLAG-mRuby3-STIM1ct showed larger distribution fractions throughout the cytosol (Fig. 1C). This correlation between oligomerization state (Fig. 1B) and membrane translocation efficiency required for Orai1-activation (Fig. 1C) was further manifested in the different efficiency of different STIM1ct fusion proteins to activate calcium-dependent gene expression; whereas ectopic overexpression of monomeric mCherry-STIM1ct and mRuby3-STIM1ct resulted in relatively poor activation of reporter gene expression from synthetic nuclear factor of activated T-cells (NFAT) promoters in human cells, EGFP-STIM1ct and AG-STIM1ct showed clear dose-dependent activation of calcium-specific transcription (Fig. 1A, D). A similar dose-dependent activation pattern for calcium-specific transcription was also observed when the fluorescent protein domains fused to STIM1ct was exchanged into other oligomeric proteins. Whereas dimeric GCN4-STIM1ct showed modest activation efficiency of calcium-dependent gene expression (GCN4 is a yeast-derived leucine zipper domain that forms a parallel coiled coil dimer)[27], fusion of STIM1ct to a 24-mer domain derived from the human ferritin gene (FTH1)[28] resulted in higher levels of target gene expression (Fig. 1E). Taken together, these results support the design principle of synthetic oligomer-dependent CRAC channel activators, where an N-terminal effector domain can propagate its oligomerization state onto the entire STIM1ct-containing molecule to directly govern its membrane translocation capability and Orai1-activation efficiency (Fig. 1A).

Bipartite CRAC activators for protein-protein interactions (PPI)-mediated reconstitution of oligomeric STIM1ct

Following the working model of oligomerization-dependent Orai1-activation described above (Fig. 1A), a most intuitive strategy to design trigger inducible CRAC activators would depend on conditional oligomerization systems where the presence of an input signal can selectively toggle a target protein between a basal monomeric state and an oligomeric conformation. For example, such approach has been previously utilized to build a optogenetic Orai1 activator called OptoSTIM1, which capitalizes on a unique blue light-dependent photolyase homology region of *Arabidopsis* cryptochrome 2 (CRY2) fused to STIM1ct, resulting in light-dependent CRY2 aggregation and activation of calcium influx[29]. However, this strategy is hardly generalizable to build CRAC activators responding to other input signals of interest, as other well-established conditional oligomer systems are scarce. Thus, instead of following such conventional design mindset, we chose a modular alternative by creating bipartite CRAC activators in which the STIM1ct and oligomer domains are split into two independent proteins that can be conditionally reassembled via different combinations of protein-protein interactions (PPI) (Fig. 2A). In this manner, formation of an oligomeric

https://doi.org/10.1038/s41467-025-58184-9

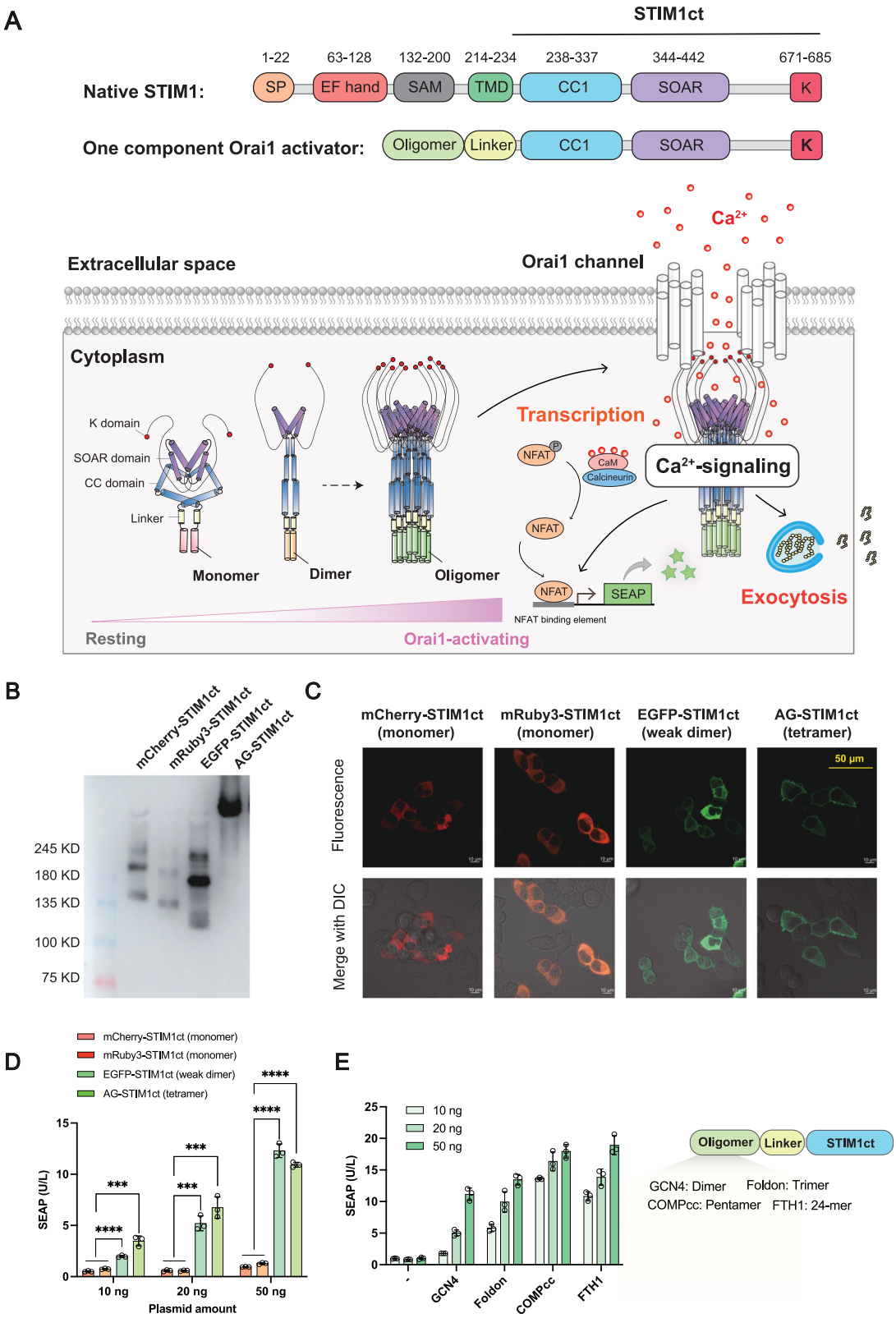

protein complex and expression of a STIM1ct-containing construct are mutually independent by design, until the presence of specific PPIs determines whether monomeric STIM1ct molecules shall join a pre-formed oligomeric "docking station" for STIM1ct aggregation, membrane translocation and Orai1-activation (Fig. 2A). Using a constitutive PPI system derived from a bacterial cohesin/dockerin interaction pair (DocS/Coh2)[30], we confirmed that oligomerization-dependent CRAC activators can indeed be separated into a split architecture to achieve a "constitutive-like" Orai1-activating conformation upon reconstitution (Fig. 2B). When Coh2-STIM1 was transfected into cells, activation of NFAT-driven target gene expression strictly required oligomeric domains (i.e. GCN4, Foldon, COMPcc or FTH1) being genetically fused to DocS, whereas co-expression of oligomeric proteins without the Coh2-specific DocS domain failed to activate calcium-dependent transcription

https://doi.org/10.1038/s41467-025-58184-9

Fig. 1 | Working model for synthetic oligomerization-dependent CRAC activators. A One component CRAC activators based on spontaneous STIM1ct oligomerization. To engineer constitutive activators of endogenous Orai1-channels, the ER-luminal part of native STIM1 was replaced by an N-terminal oligomeric protein domain, producing cytoplasmic STIM1ct proteins whose membrane translocation capability exclusively depends on its spontaneously formed oligomerization state. While fusion of monomers yields resting STIM1ct states incapable of Orai1-activation, CRAC activation efficiency directly correlates with the oligomerization status of synthetic STIM1ct. CRAC-mediated calcium influx can trigger activation of endogenous calmodulin/calcineurin-dependent nuclear factor of activated T-cells (NFAT) signaling and transcription from NFAT-specific promoters or Ca^{2+}-dependent exocytosis in secretory cell types. **B** Oligomeric state of different fluorescent STIM1ct fusion proteins. Target proteins in each lysate were detected by native PAGE. Numbers on the left axis represent molecular weights (MW) of denatured target proteins. **C** Subcellular localization of different STIM1ct fusion proteins. Fluorescent images were acquired 48 h after transfection by confocal microscopy (scale bar: 50 μm). Representative images for 3 independent experiments are shown. **D** Stimulation of Ca^{2+}-dependent gene expression by different fluorescent STIM1ct fusion proteins. **E** Ca^{2+}-dependent gene expression mediated by chimeric STIM1-oligomers. Data are presented as the mean ± SD, $n = 3$ independent experiments. Error bars = SD. Two-tailed unpaired Student t-tests were used to evaluate the statistical significance of differences between two groups. *P*-values more than 0.05 were considered statistically not significant. $^{*}p < 0.05$, $^{**}p < 0.01$, $^{***}p < 0.001$, $^{****}p < 0.0001$. Source data are provided as a Source Data file.

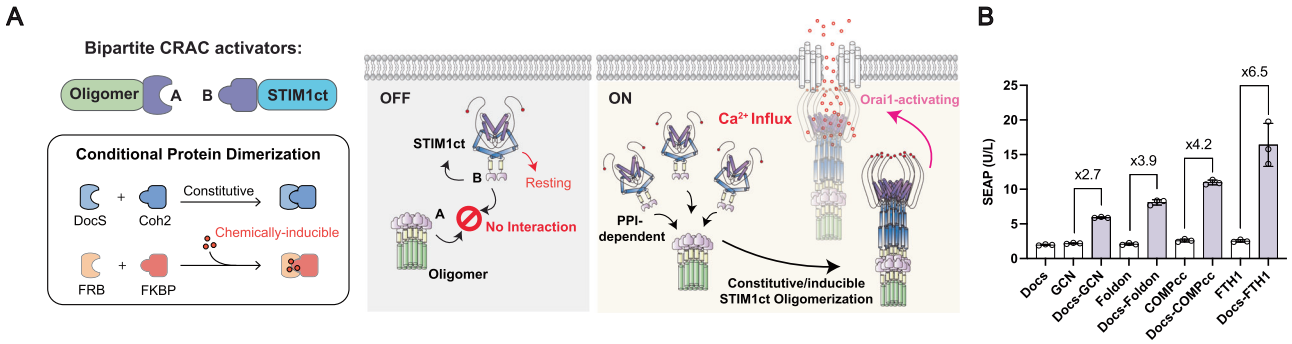

Fig. 2 | Design of bipartite CRAC activators. A Conceptual design. Synthetic CRAC activators can also be expressed as two separate proteins in which STIM1ct and the oligomeric domain are each fused to different proteins that conditionally interact with each other via constitutive or chemically-inducible protein-protein interactions (PPI). In the absence of PPI, STIM1ct cannot interact with the oligomeric complex and therefore remains in a resting state. Only pre-programmed PPI events can allow individual STIM1ct molecules to join an oligomeric "docking station", resulting in STIM1ct oligomerization and Orai1 activation. **B** Experimental validation by Ca^{2+}-dependent gene expression. Source data are provided as a Source Data file. Numbers indicate average fold-changes of SEAP expression within column groups.

(Fig. 2B). This result confirms the mode of action of bipartite CRAC activators and suggests that trigger-inducible CRAC activators could be engineered through modular exchange of the constitutive DocS/Coh2 interaction into conditional protein dimerization pairs[31,32] (Fig.2A).

Trigger-inducible CRAC activators to monitor Ca^{2+}-influx using clinically licensed small molecule drugs

Regulation of therapeutic transgene expression using clinically-licensed small molecules is essential to improve safety profiles of cell-based therapies in vivo[2,9]. A classical example of an FDA-approved trigger compound for regulation of gene and cell-based therapies is rapamycin, which induces dimerization of the FKBP/FRB protein pair[33]. To test whether this chemically-induced dimerization (CID) system can be "plugged" into the framework of bipartite CRAC activators (Fig. 2A), we created various constructs with STIM1ct fused to either FRB (pLYL295, P_{hCMV}-FRB-STIM1ct-pA) or FKBP (pLYL296, P_{hCMV}-FKBP-STIM1ct-pA) and co-expressed FRB-STIM1ct or FKBP-STIM1ct with corresponding Foldon- or FTH1-based oligomeric proteins (pLYL298, P_{hCMV}-FKBP-Foldon-pA; pLYL331, P_{hCMV}-FKBP-FTH1-pA; pLYL297, P_{hCMV}-FRB-Foldon-pA; pLYL330, P_{hCMV}-FRB-FTH1-pA) (Fig. 3A). Results show that most combinations permitted rapamycin-dependent Orai1 activation, with FKBP-STIM1ct and FRB-FTH1 showing highest fold-changes of calcium-dependent gene expression as evaluated with the NFAT-specific reporter assay (Fig. 3A).

Minimization of side effects potentially elicited by the control compound is another factor that must be carefully considered when developing cell-based therapies for clinical usage[9]. Though rapamycin shows excellent performances in regulating gene expression upon reconstitution of Orai1-activating STIM1-configurations at a cellular level (Fig. 3A), administration of rapamycin or its analogues to patients still bears substantial risks of adversely inhibiting mammalian target of rapamycin (mTOR) pathways in unrelated cells or tissues[34]. Therefore, from a clinical perspective, viral inhibitors are increasingly being regarded as ideal control compounds for gene- and cell-based therapies, since this class of drugs not only have well-studied safety and pharmacokinetics profiles, but most importantly do not target human proteins[2,9,34]. For example, grazoprevir is a clinically-licensed drug to treat Hepatitis C virus (HCV), and triggers chemically-induced dimerization between the HCV-specific protease NS3a and a de novo designed GNCR1 protein at picomolar affinity[35]. Thus, to increase clinical eligibility, we created a grazoprevir-regulated CRAC activator by substituting the rapamycin-dependent FKBP/FRB system with the NS3a/GNCR1 pair (Fig. 3B). Then, using an analogous combinatorial approach to test various STIM1ct-, Foldon- and FTH1-domains fused to NS3a or GNCR1 as previously shown for the rapamycin-based system, co-expression of NS3a-STIM1ct and GNCR1-FTH1 was established as the bipartite CRAC activator that permitted highest dynamic ranges of fold-induction in terms of grazoprevir-inducible expression of calcium-dependent genes (Fig. 3B). Indeed, all combinations caused a rapid surge of intracellular Ca^{2+} within 2–3 min upon grazoprevir administration, thus confirming the proposed mechanistic link between the individual panels of trigger-inducible STIM1 assembly, oligomerization-dependent membrane translocation, calcium influx and target gene expression (Fig. 3C). Furthermore, we showed that grazoprevir-mediated calcium influx was indeed dependent on the activity of endogenous CRAC channels (Figure S1), that the amount of Ca^{2+}-dependent gene expression could be precisely fine-tuned by different grazoprevir doses (Fig. 3D), and that grazoprevir-dependent CRAC stimulation neither causes signs of apoptosis (Figure S2) nor significant alterations of endogenous gene expression in the host cell (Figure S3).

Grazoprevir-inducible Ca^{2+} influx can boost endogenous hormone release in endocrine cells

Achievement of on-demand drug release is a long-standing goal of modern cell-based therapies[36]. Thus, after establishing an "upstream" module capable of mediating trigger-inducible Ca^{2+}-influx in various

https://doi.org/10.1038/s41467-025-58184-9

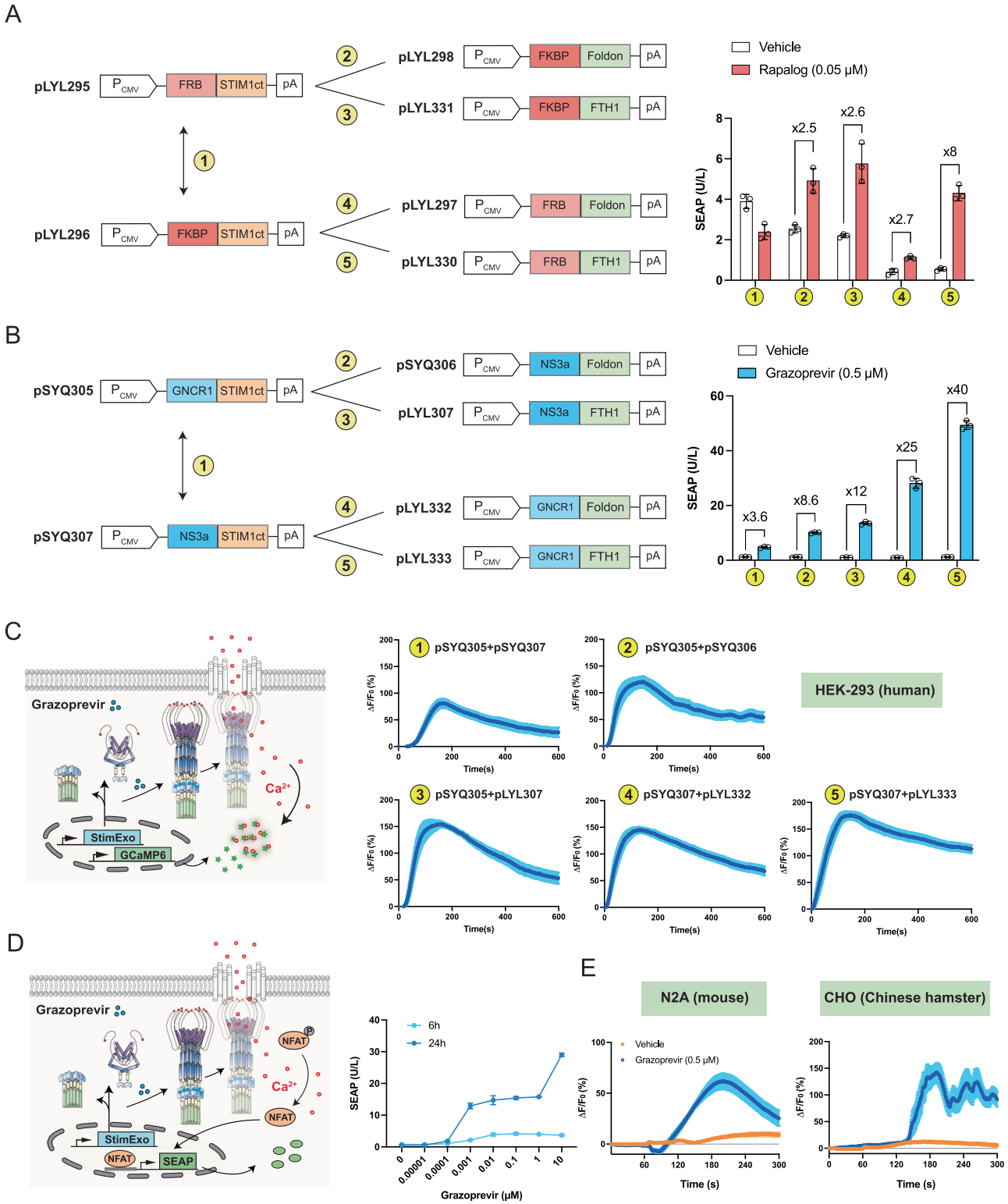

Fig. 3 | Design and construction of drug-inducible CRAC activators. A Calcium-dependent gene expression by rapalog-triggered STIM1 assembly. **B** Calcium-dependent gene expression by grazoprevir-triggered STIM1 assembly. **C** Visualization of grazoprevir-triggered calcium influx. **D** Dose-dependence of grazoprevir-inducible SEAP expression. **E** Grazoprevir-triggered calcium influx in various cell lines. Data in (**A**, **B**, **D**) are presented as the mean ± SD, $n = 3$ independent experiments. Error bars = SD. Data in (**C**) are presented as mean ± SEM, $n = 3$ independent experiments. Error bars = SD. Source data are provided as a Source Data file.

mammalian or human cell types (Fig. 3E), we next sought to build a synthetic excitation-secretion pathway by providing a link between grazoprevir-inducible CRAC activation and protein exocytosis (Fig. 4A). In humans, many peptide hormones with therapeutic value are stored within secretory granules of endocrine cells, which rapidly release their cargo following surges of intracellular Ca^{2+} [37,38]. To test whether grazoprevir-regulated CRAC activation can trigger endogenous hormone release, we transiently transfected the genetic components for StimExo (NS3a-STIM1ct and GNCR1-FTH1) into B16-F10 cells, a dermal cell line isolated from a murine melanoma model.

https://doi.org/10.1038/s41467-025-58184-9

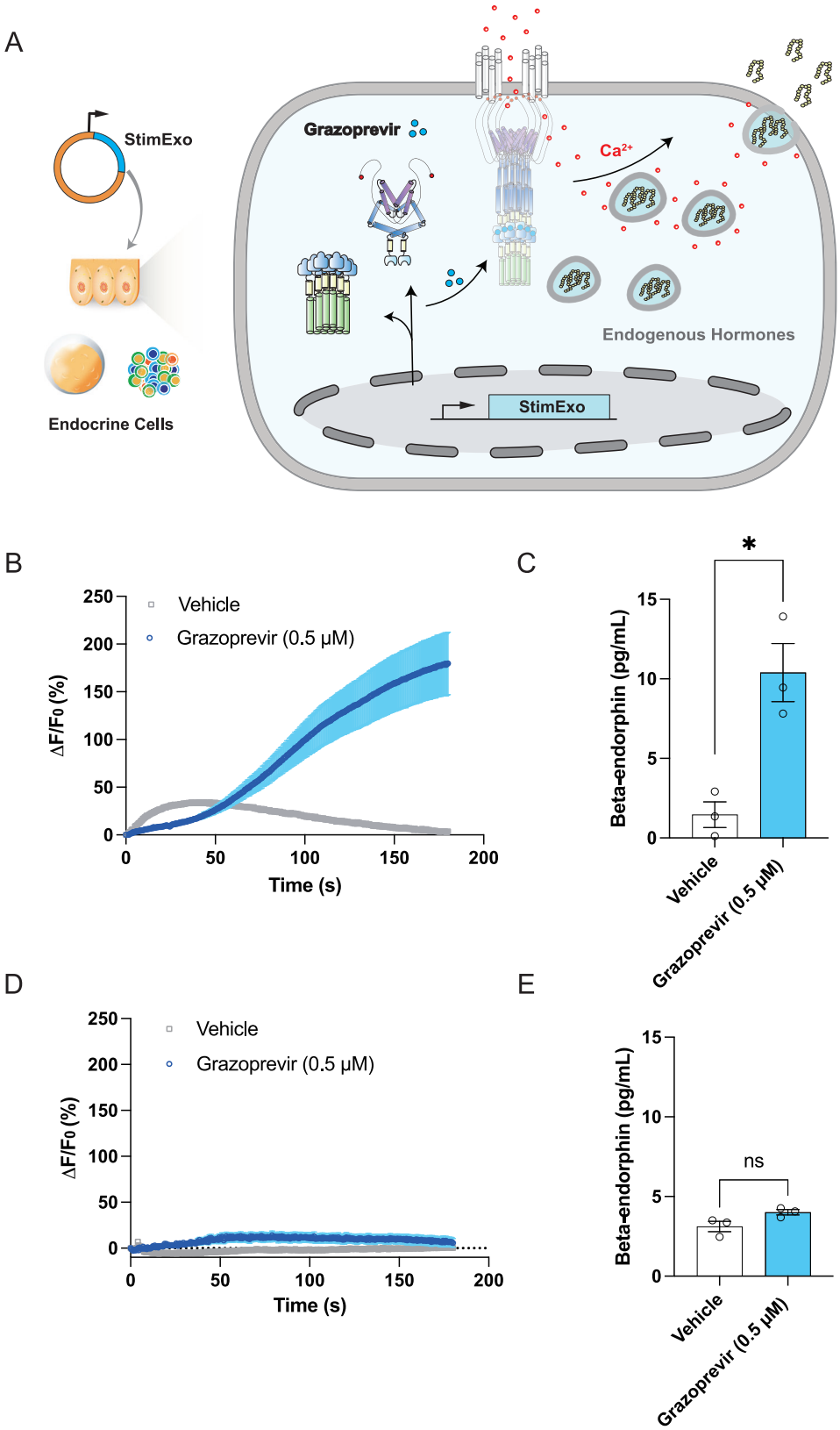

Fig. 4 | Grazoprevir-triggered release of therapeutic hormones in endocrine cells. A Schematic illustration. Application of trigger-inducible Orai1 activators into secretory endocrine cell types allows different user-defined trigger signals of interest (e.g., Grazoprevir) to monitor instant calcium influx and stimulate exocytosis of cell type-specific therapeutic hormones. **B** Grazoprevir-triggered calcium influx in B16-F10 cells. **C** Grazoprevir-triggered secretion of β-endorphin. **D** Grazoprevir-triggered calcium influx in native B16-F10 cells. **E** Grazoprevir-triggered secretion of β-endorphin in native B16-F10 cells. Data in (**B**, **D**) are presented as mean ± SEM, $n = 10$ different cells. Error bars=SEM. Data in (**C**, **E**) are presented as mean ± SEM, $n = 3$ independent experiments. Error bars=SEM. Two-tailed unpaired Student t-tests were used to evaluate the statistical significance of differences between two groups. *P*-values more than 0.05 were considered statistically not significant. $^{*}p < 0.05$, $^{**}p < 0.01$, $^{***}p < 0.001$, $^{****}p < 0.0001$. Source data are provided as a Source Data file.

In fact, skin is an unconventional endocrine organ whose hormone production ability is largely neglected[39]. In particular, melanocytes, keratinocytes, dermal fibroblasts and endothelial cells were all reported to synthesize and secrete large amounts of β-endorphin - an opioid neuropeptide with functions related to stress reduction and maintenance of energy homeostasis[40]. When we introduced StimExo into B16-F10 cells, grazoprevir indeed triggered intracellular Ca^{2+} elevation (Fig. 4B) and concomitant secretion of β-endorphin within 15 min (Fig. 4C). In contrast, grazoprevir-inducible Ca^{2+} influx and β-endorphin release were not observed in native B16-F10 cells not expressing StimExo (Fig. 4D, E). Therefore, StimExo can be potentially applied as a "genetically encoded secretagogue" to boost endogenous hormone release in specialized human cell types. For future implementation, such treatment concept could either utilize AAV-based gene delivery of StimExo components into targeted tissues or organs to achieve on-demand protein secretion in a gene therapy setting, or applied to patients via cell-based delivery strategies as we will discuss next.

A generalizable drug-inducible exocytosis pathway for on-demand secretion of various therapeutic outputs of interest

Next, we show that StimExo-mediated protein exocytosis is also applicable to pancreatic host cells for treatments that are related, but not limited to type-1 diabetes. For vesicular secretion of various proteins of interest (POI), the proinsulin backbone can be used as a versatile expression system in various endocrine cell types. Proinsulin comprises three polypeptide fragments known as B-, C- and A-chains in its genetically encoded amino acid order. In pancreatic β-cells, the proinsulin molecule is delivered into secretory granules for post-translational maturation, which occurs through proteolytic cleavage and removal of the C-peptide part, followed by formation of stabilizing disulfide bridges between B-chains and A-chains. Thus, upon calcium-dependent exocytosis, mature insulin (only comprising B- and A-chains) and therapeutically inactive C-peptide are co-secreted in an equimolar ratio. To use this pathway to secrete other output proteins of interest, the C-peptide part of proinsulin can be exchanged into an arbitrary genetic sequence encoding for any other POI, therefore allowing vesicular POI secretion by utilizing the native exocytotic machinery of insulin[41] (Fig. 5A). Indeed, such strategy was employed in some former studies, for example by selecting a monoclonal cell line ElectroBeta stably transgenic for co-secretion of insulin and luciferase[19] (Fig. 5B), or by introducing point mutations into B- and A-chain residues to create insulin-deficient expression systems for exclusive secretion of diabetes-unrelated output proteins[18,42]. Furthermore, it has been previously shown that activation of CRAC channels can indeed stimulate insulin exocytosis in pancreatic cells[43]. Here, we wondered whether grazoprevir-triggered Ca^{2+} influx mediated by StimExo is also compatible with this generalizable exocytosis strategy (Fig. 5A). For proof-of-concept, different StimExo variants (NS3a-STIM1ct co-expressed with either GNCR1-FTH1, GNCR1-COMPcc or GNCR1-Foldon; compare Fig. 2B) were stably expressed in glucose- and grazoprevir-insensitive ElectroBeta cells (Fig. 5C). Surprisingly, the NS3a-STIM1ct/GNCR1-FTH1 combination accounting for high performances in our previous experiments failed to trigger POI exocytosis in ElectroBeta cells (Fig. 5C), potentially due to some unknown cellular background of this pancreatic host cell prohibiting proper FTH1 expression. Qualitatively, we show that the efficiency of FTH1-dependent constructs to form the expected 24-mer aggregation state was indeed relatively low in ElectroBeta cells – irrespective whether grazoprevir was supplied or not (Figure S4). Instead, grazoprevir-dependent exocytosis was observed with the NS3a-STIM1ct/GNCR1-Foldon combination (Fig. 5C), which was also effective in forming higher-order oligomeric states in HEK-293 cells (Figure S4). Thus, stable expression of NS3a-STIM1ct and GNCR1-Foldon in ElectroBeta cells allowed for dose-dependent grazoprevir-triggered exocytosis within a few minutes, with peak amounts of target protein release being recorded within the 1st hour following stimulation with grazoprevir (Fig. 5D). Furthermore, we showed that basal exocytosis rates in the grazoprevir-absent OFF-state were not affected by fluctuations of extracellular Ca^{2+} levels, while higher amounts of extracellular Ca^{2+} could improve grazoprevir-stimulated exocytosis rates (Figure S5). These results confirm the feasibility of using StimExo variants to precisely control protein exocytosis from a customizable proinsulin-based vesicular system.

Real-time control of blood glucose homeostasis by a cell-based therapy approach of grazoprevir-triggered insulin exocytosis

Lastly, we sought to capitalize on the grazoprevir-triggered insulin exocytosis system and describe a clinically eligible cell therapy approach for treatment of type-1 diabetes (Fig. 6A), an autoimmune disorder characterized by insulin deficiency and chronically elevated blood glucose levels[44]. Thus, after confirming the feasibility of achieving grazoprevir-dependent exocytosis in ElectroBeta cells (Fig. 5D), we used a Sleeping Beauty transposase based selection strategy[45] to engineer monoclonal cell lines with superior fold-changes of insulin production (Figure S6). Among 25 individual cell clones harvested and validated, a clone labeled as 2-E8 showed the best profile of grazoprevir-dependent NanoLuc production, which we designated as "StimExoINS" (Figure S6). Notably, because the proinsulin backbone allows co-secretion of insulin and NanoLuc in an 1:1 ratio (Fig. 5A), the luciferase readout reflecting effective insulin levels is a practical tool for such high-throughput screens, given that conventional insulin assays would generate significantly higher costs and overall labor[41]. Indeed, monoclonal StimExoINS cells showed an almost identical profile between grazoprevir-dependent NanoLuc (Fig. 6B) and insulin (Fig. 6C) secretion, permitting long-term and reversible control of grazoprevir-stimulated exocytosis (Figure S7) and showing a typical kinetic profile of calcium-dependent exocytosis following stimulation with either potassium chloride (triggering membrane depolarization) or grazoprevir (triggering CRAC activity) (Fig. 6D). Next, we encapsulated StimExoINS into coherent immune-isolating alginate-poly-L-lysine-alginate microbeads (Fig. 6A), a clinically eligible delivery method for stem cell-based diabetes therapies[46]. Notably, exocytosis efficiency appears to significantly depend on the molecular weight of the chosen poly-L-lysine (PLK) material (Fig. 6E). Whereas grazoprevir-dependent NanoLuc secretion was diminished when using PLK of higher molecular weight, PLK of lower molecular weight (e.g., 2100 Da) producing more "flocculent" microbeads permitted optimal diffusion efficiency of trigger signals (e.g. grazoprevir) and output proteins (e.g. insulin and NanoLuc) across the capsule membranes (Fig. 6E, F). Upon implantation of microencapsulated StimExoINS cells into mice, we show that administration of 1 mg/kg resulted in optimal activation of target protein secretion within minutes (Fig. 6G). Notably, the bioavailability of grazoprevir in vivo (maintaining high plasma concentrations during the first 2-3 hours after administration; Figure S8) appeared to be compatible with timescale of the grazoprevir-dependent exocytosis system, which releases most of its insulin content within a few minutes post stimulation (Fig. 6D) and may reach saturating levels of target protein secretion within 4 h (Fig. 5D). These parameters are critical to ensure that insulin is instantly secreted into the bloodstream of mice soon after grazoprevir uptake (Figure S9A), but therapeutic effects are also rapidly terminated as soon as the mice are no longer stimulated with the working dose(s) of the trigger signal. Indeed, when testing different cell implants in type-1 diabetic mice, only microencapsulated StimExoINS cells enabled real-time control of blood glucose homeostasis following treatment with 1 mg/kg grazoprevir, whereas administration of grazoprevir alone or implantation of parental ElectroBeta cells failed to regulate glycemia (Fig. 6H). Glucose tolerance of type-1 diabetic mice was also improved by grazoprevir-mediated stimulation of StimExoINS in vivo (Figure S9B). Importantly,

https://doi.org/10.1038/s41467-025-58184-9

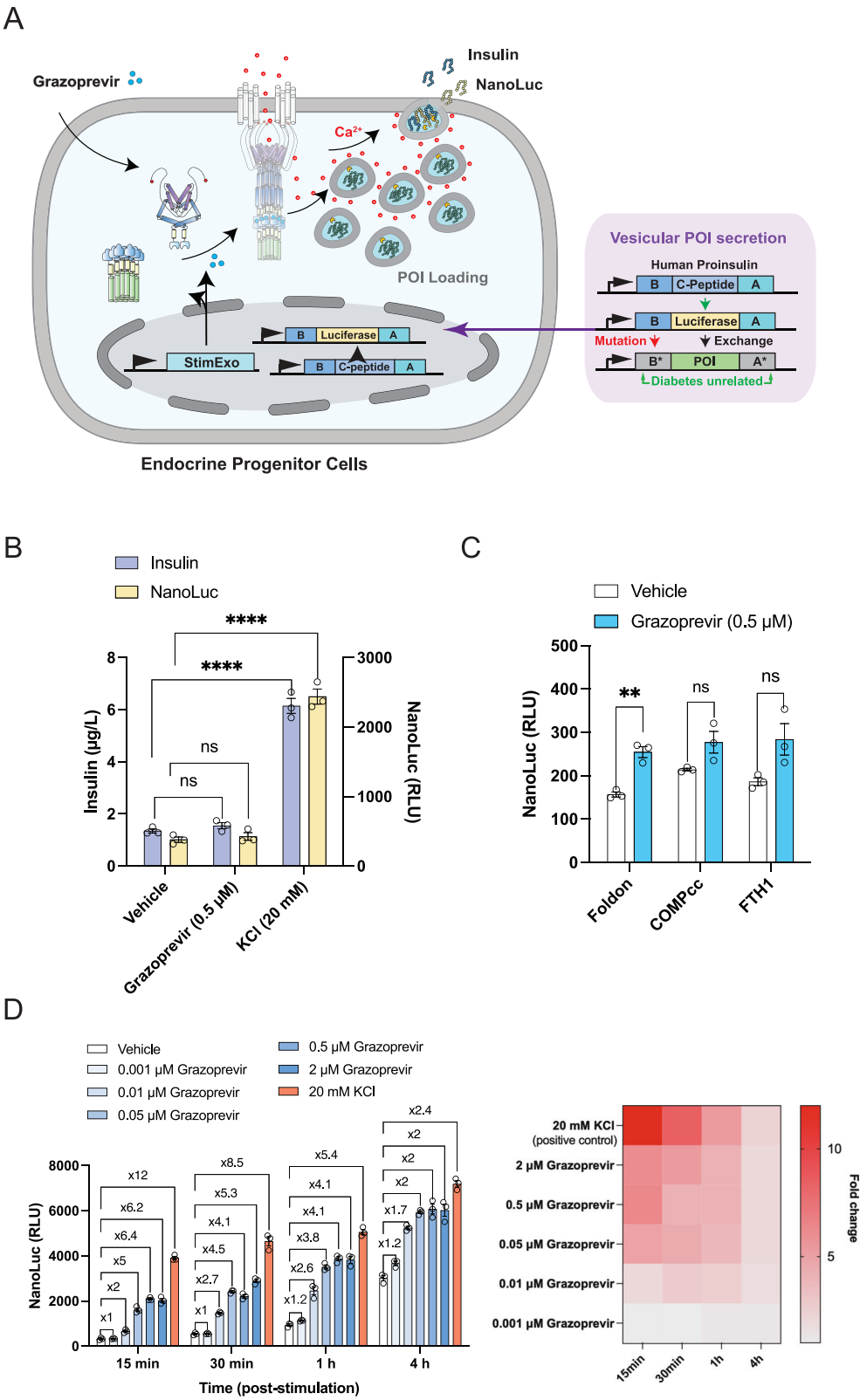

Fig. 5 | Trigger-inducible exocytosis of various target proteins of interest. **A** Schematic illustration. In secretory cell types, the proinsulin backbone can be used as an expression system to allow various proteins of interest (POI) to utilize the Ca^{2+}-dependent exocytosis pathway of native insulin. By exchanging the C-peptide segment of proinsulin by a gene sequence encoding for the POI, various proteins of interest (POIs) can be loaded into the secretory granules of insulin and secreted upon (grazoprevir-dependent) stimulation of Ca^{2+}-influx. For application unrelated to diabetes, B- and A-chains of insulin can be further mutated to attenuate glycemic (side-) effects. **B** Calcium-dependent exocytosis of native ElectroBeta cells. **C** Comparative analysis of different ElectroBeta cell lines stably transgenic for grazoprevir-inducible exocytosis. **D** Dose-dependent fold-changes of NanoLuc secretion. Heatmap shows the average fold-changes calculated by dividing NanoLuc levels of Grazoprevir- or KCl-treated samples by basal NanoLuc levels of samples treated with native RPMI medium. Data in (**B**–**D**) are presented as the mean ± SEM, $n = 3$ independent experiments. Error bars=SEM. Two-tailed unpaired Student t-tests were used to evaluate the statistical significance of differences between two groups. *P*-values more than 0.05 were considered statistically not significant. $^{*}p < 0.05$, $^{**}p < 0.01$, $^{***}p < 0.001$, $^{****}p < 0.0001$. Source data are provided as a Source Data file.

https://doi.org/10.1038/s41467-025-58184-9

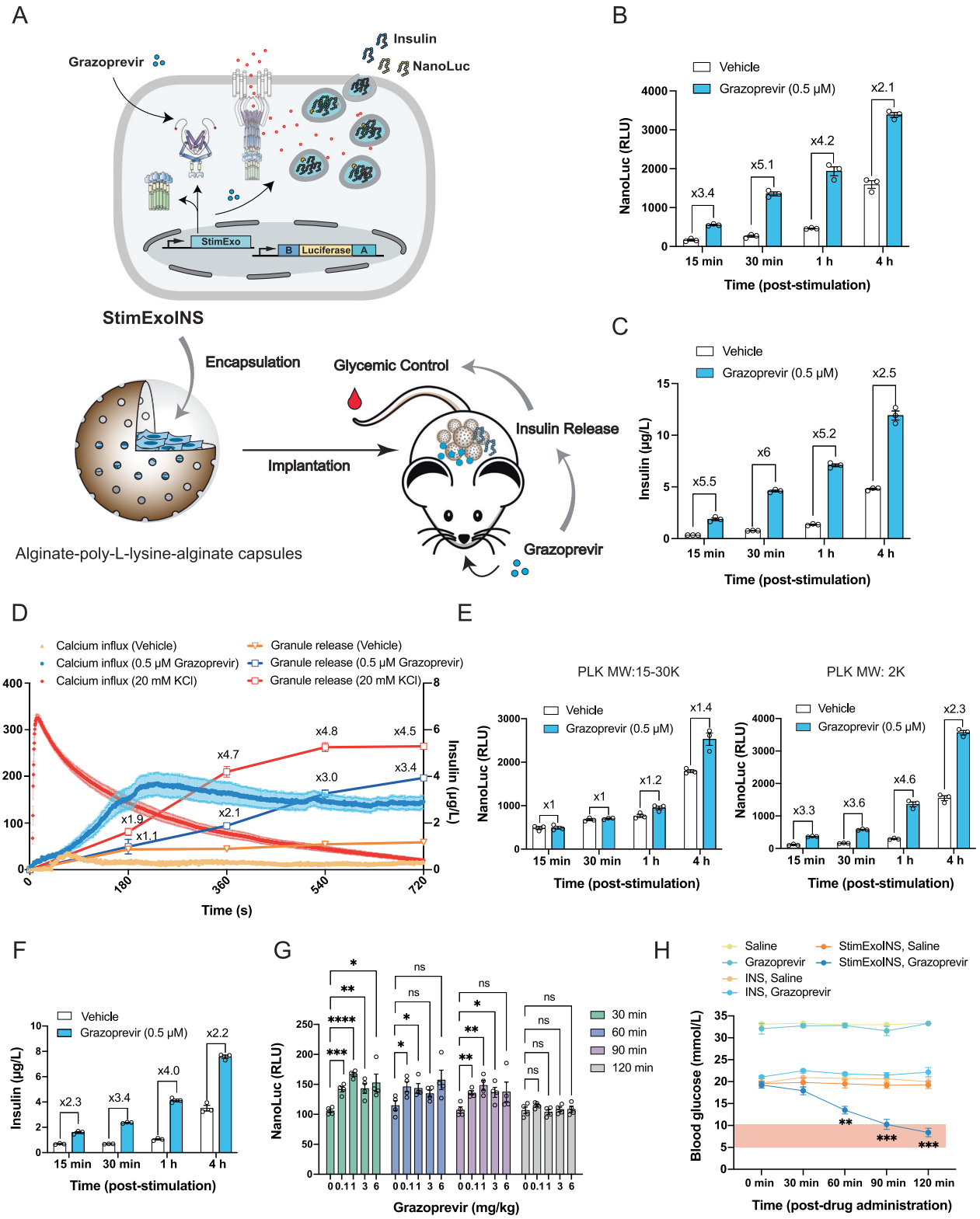

no hypoglycemic excursions were observed throughout our studies following grazoprevir discontinuation (Fig. 6H & Figure S9B). Therefore, StimExoINS can effectively mediate on-demand secretion of therapeutic protein in cell therapy settings for future treatments of metabolic disorders that critically require instant drug actions.

Discussion

Currently, cell-based therapies are rapidly progressing through clinical trials and regulatory approval[47,48]. By designing sophisticated gene circuits capable of precisely controlling spatial, temporal and dose-dependent therapeutic regimen of implanted cells, synthetic biology seeks to significantly advance modern gene- and cell-based therapies and enable treatment opportunities for many intractable human diseases[1,9]. For example, gene circuits allowing endogenous disease markers of a patient to directly modulate therapeutic transgene expression often yield fully autonomous therapeutic algorithms, where diagnosis, treatment and prevention of a pathologic situation are self-sufficiently coordinated in closed-loop[4,49]. However, a

Fig. 6 | Real-time control of blood glucose homeostasis by grazoprevir-inducible insulin exocytosis in type-1 diabetic mice. A Principles of a StimExoINS-mediated cell therapy. Pancreatic host cells stably transgenic for StimExo and insulin expression (StimExoINS) are encapsulated into semipermeable alginate-poly-L-lysine-alginate beads and implanted into type-1 diabetic mice. Insulin exocytosis triggered by grazoprevir administration enables instant regulation of blood glucose levels. **B**, **C** Kinetics of grazoprevir-triggered insulin exocytosis in monoclonal StimExoINS cells. **D** Kinetics of calcium-dependent insulin exocytosis. **E**, **F** Grazoprevir-triggered exocytosis in microencapsulated StimExoINS cells. Same volume of alginate microbeads containing monoclonal 2-E8 cells generated with poly-L-lysine (PLK) of different molecular weight (MW) were seeded in 1 mL serum-free RPMI medium (vehicle control) or RPMI medium containing 0.5 μM Grazoprevir before NanoLuc levels in culture supernatants were profiled at different timepoints (**E**). insulin levels of PLK (MW:2000) microbeads were also quantified at different timepoints (**F**). Data in (**B**–**F**) are presented as the mean ± SEM, $n = 3$ independent experiments. Error bar=SEM. **G** Quantification of grazoprevir-inducible exocytosis in vivo. One day after implantation of 5×10^6 microencapsulated 2-E8 cells into 8-week healthy wildtype *C57/BL6J* male mice, animals received different doses of grazoprevir solutions via intraperitoneal injection. NanoLuc production in the bloodstream was measured every 30 min. **H** Real-time glycemic control by grazoprevir-triggered insulin exocytosis in diabetic mice. 1 day after intraperitoneal implantation of 1×10^7 microencapsulated StimExoINS or ElectroBeta into T1DM mice, mice were fasted for 4 h and received single injections of 200 μL saline (vehicle control) or grazoprevir (1 mg/kg) before glycemic levels were followed over 120 min. T1DM mice receiving grazoprevir but no cell implants were used as negative controls. Homeostatic blood glucose levels (5-10 mM) are marked with a transparent red box. Data in (**G**, **H**) are presented as the mean ± SEM; $n = 4$ mice per group, Error bar = SEM. Two-tailed unpaired Student t-tests were used to evaluate the statistical significance of differences between two groups. *P*-values more than 0.05 were considered statistically not significant. $^*p < 0.05$, $^{**}p < 0.01$, $^{***}p < 0.001$, $^{****}p < 0.0001$. Source data are provided as a Source Data file.

completely self-operating system may face safety and unpredictability concerns when used in a clinical setting. Therefore, engineering of "open-loop" regulation layers that allow external trigger compounds to remote control and/or intervene therapeutic transgene expression within patients are gaining increased attention[2].

Recently, physical cues such as temperature[18], electricity[19] or light[20,43] were proposed as promising strategies for remote control of transgene activities due to a theoretically traceless and non-invasive nature of the trigger signal[50]. Indeed, some of such systems have also been developed to trigger protein exocytosis for cell therapy applications, for example through ectopic expression of light-sensitive cell surface receptors or voltage-gated ion channels into pancreatic beta cells[19,20]. However, many of those physically regulated systems require special attention and sometimes additional engineering efforts for application in a real-world setting. For example, light and temperature are ubiquitous environmental signals that are impossible to selectively avoid in daily life[51]. In addition, cell therapies based on these systems are mostly prefer subcutaneous implantation, as the penetration efficiency of these trigger signals to the circulation or other internal organs is relatively poor[52]. Thus, application of this class of therapies often requires specialized hardware for cell delivery, such as macroencapsulation techniques containing electronic controllers[19] or even wirelessly powered LED devices co-implanted alongside the engineered cells in vivo[52]. Therefore, for practical and regulatory reasons, a safe, patient compliant and FDA-approved small molecule trigger with clinically validated pharmacokinetics (PK) profiles is increasingly been regarded as an ideal trigger compound for cell therapy control[2]. Specifically, antiviral drugs fulfill almost all criteria for a clinically-eligible trigger compound because many of these drugs have favorable PK and safety profiles with no endogenous human target, which is fundamental to avoid potential on-target pharmacology by endogenous metabolites or any other off-target effects of the drug[9,34].

In this work, we therefore chose grazoprevir, an FDA-approved drug against Hepatitis C virus, as the prime molecular trigger to showcase potential cell therapy applications of StimExo. Evidently, ligand-responsiveness is not limited to the trigger compounds that we have shown in this work - as activation of calcium release activated Ca^{2+} (CRAC) channels and calcium-dependent exocytosis can be flexibly adjusted to respond to any other signal of interest through exchange of the grazoprevir-inducible NS3a:GNCR1 module or the rapalog-inducible FRB:FKBP module into other established PPI system without causing significant toxicities related to aberrant Ca^{2+} entry (Figure S2)[53]. This kind of modularity is a key advantage over some conventional synthetic regulators of STIM1 activity. For example, OptoSTIM is a popular tool widely adopted for mechanistic studies of neuroscience[54,55] and immunology[56], which capitalizes on direct fusion of light-inducible oligomeric CRY2-domain to the cytoplasmic STIM1ct domain[29]. Upon light illumination, oligomerization of CRY2 yields the Orai1-activating conformation of STIM1, resulting in light-dependent calcium influx. Though OptoSTIM systems are also compatible with activation of calcium-dependent exocytosis in iPSC-derived pancreatic organoids[43], repurposing of the light-specific OptoSTIM design to engineer an analogous system responding to another trigger compound (such as small molecule drugs) would be technically more demanding than with StimExo. To change a trigger compound, the light-inducible oligomeric CRY2-domain must be exchanged by a conditional oligomerization system regulated by the new signal of interest (e.g., grazoprevir). Unlike protein dimerization systems[53], chemically-inducible oligomers are less extensively catalogued in the field. Therefore, to achieve generalizable input signal sensing, StimExo can build on a vast repertoire of well-characterized PPI systems by design, rather than relying on the availability of naturally evolved cell surface proteins coupling to calcium signaling[18–20] or compatible oligomeric systems responding to the specific trigger signal of interest[29,43]. Notably, the extent of trigger-inducible STIM1 activation may remain at similar non-toxic ranges of physiological CRAC activities, which may warrant additional safety when moving towards therapeutic applications.

Taken together, StimExo was designed to overcome a key limitation factor that was prohibiting instantaneous "sense-and-secrete" cell-based therapies, eventually allowing any user-defined input signal of interest to trigger protein exocytosis. Notably, all molecular parts of StimExo were carefully chosen to be eligible for clinical use, i.e., the genetic components are either human-derived or minimally xenogeneic[9]. Furthermore, we used the clinically-licensed drug grazoprevir as a safe and patient-compliant trigger compound that is orthogonal to the human metabolism[9]. This will minimize undesired pharmacological effects upon drug exposure, especially when compared to conventional rapamycin-regulated gene therapies[34]. StimExo is also simple in design and achieves trigger-inducible protein secretion without the need to incorporate exogenous proteases[57–59], which is another important factor when developing gene and cell-based therapies towards clinical consideration[9,60]. Lastly, with alginate microencapsulation being a clinically eligible cell delivery route for type-1 diabetes treatment[61], a StimExoINS-enabled cell therapy concept may provide a valuable gene circuit asset for future diabetes therapies. Currently, we demonstrate proof-of-principle of grazoprevir-inducible insulin exocytosis by introducing the genetic componentry of StimExo into ElectroBeta – an insulin-deficient und glucose-insensitive pancreatic cell line engineered for stable expression of proinsulin[19]. For clinical usage, a non-tumorigenic cell type should be preferentially chosen as the final chassis for StimExo, albeit alginate microbeads can theoretically prohibit any leakage of its encapsulated cellular content into the circulation[62]. Similarly, the optimal dosing and administration route of the trigger compound remains to be determined in future work. Here, we could effectively

control target protein exocytosis using a grazoprevir dose of 0.1–1 μM in vitro and in mice following intraperitoneal injection (Figure S8B). For translation towards clinical applications in humans, more reliable and patient-compliant administration routes (e.g., sublingual delivery) that may enable even higher grazoprevir sensitivities (e.g., in the low nanomolar range) must be the goal of future development. Thus, in case these questions are adequately addressed in the not-too-distant future, a new alternative for diabetes treatment can thus be developed based on simple overexpression of StimExo and proinsulin genes in a safe and clinically eligible secretory host cell. When compared to conventional approaches relying on differentiation of pancreatic beta-cells from stem cells[63], an engineering-driven approach through introduction of synthetic gene circuits into certified chassis lines would be advantageous in terms of manufacturability, scalability and product specificity. In this with this, StimExo has the potential to provide a technological platform to engineer cell therapies to treat diabetes and many other metabolic diseases that require instant and on-demand drug secretion within patients.

Methods

Vector design

Construction details and references for all expression vectors are provided in Table S1. Related sequences are provided in Supplementary Data 1. New plasmids were generated using standard restriction and digestion cloning (New England Biolabs; Beverly, MA) or In-Fusion cloning techniques (ClonExpress MultiS One Step Cloning Kit). PCR-amplification reactions were performed using KOD One PCR Master Mix. Ligation was performed using T4 DNA Ligase. DNA was extracted with TIANGEN plasmid miniprep kit. Constructs were verified by sequencing service of Tsingke Biotechnology (Beijing, China). Primers were synthesized by Tsingke Biotechnology.

Chemical and reagents

All consumables used and purchased for this study are listed in Table S3. Chemical stock solutions are listed in Table S4. Buffer preparation information are provided in Table S5.

Cell culture

Human embryonic kidney cells (HEK-293; ATCC: CRL-11268) and murine neuroblasts (N2A; ATCC: CCL-131) were cultivated in Dulbecco's modified Eagle's medium (DMEM) supplemented with 10% CellMax Fetal Bovine Serum (FBS) and 1% (v/v) penicillin/streptomycin solution (PenStrep). Murine melanoma (B16-F10; ATCC: CRL-6475), ElectroBeta[19] and derivative cell lines were cultivated in Roswell Park Memorial Institute 1640 Medium (RPMI medium) supplemented with 10% FBS and with 1% PenStrep. Chinese hamster ovary cells (CHO; ATCC: CCL-61) were cultivated in Ham's F-12K (Kaighn's) medium supplemented with 10% FBS and with 1% PenStrep. All cells were cultured at 37 °C in a humidified atmosphere of 5% CO_2 in air. For passaging and cell culture, cells of pre-confluent cultures were detached by incubation in 0.05% Trypsin-EDTA for 3 min at 37 °C, collected in 10 ml of cell culture medium, centrifuged for 2 min at 1000 rpm (or 3 min at 200 g), and resuspended in fresh culture medium at a standard density of 1.5×10^5 cells/mL before seeding into new tissue culture plates. Cell number and viability were quantified using an AMQAX1000 COUNTESS II Cell counter (ThermoFisher Scientific; Waltham, MA).

Transfection of mammalian cells

Unless indicated otherwise, transient transfection was performed at 24 h after seeding 50'000 mammalian cells into each well of a 24-well plate. pcDNA3.1(+) (Invitrogen, CA; cat-no. V79020) was used as a filler plasmid to keep total DNA amounts constant (500 ng). HEK-293 were transfected using an 1 g/L aqueous Polyethyleneimine (PEI) solution-based protocol at a PEI:DNA ratio of 4:1 (w/w) and in a transfection volume of 50 μL Minimum essential medium MEM per well. B16-F10, N2A, ElectroBeta and derivatives were transfected using Lipofectamine 3000 reagent according to the manufacturer's instructions. CHO cells were transfected using Lipofectamine 2000 reagent according to the manufacturer's instructions. Transfection agents and nucleic acids were incubated for 15 min at 25 °C before dropwise addition to cells. The cell culture medium was replaced with fresh medium (not containing transfection reagents) at 6 h after transfection.

Generation of stable cell lines

Polyclonal Electro-FTH1, Electro-FTH1(3xFLAG), Electro-COMPcc and Electro-Foldon populations, stably transgenic for constitutive expression of the genetic componentry for grazoprevir-inducible STIM1 assembly, were constructed by co-transfection of 25 ng pCMV-T7-SB100 and 500 ng pSYQ346, pLYL466, pSYQ347 or pSYQ348 into 5×10^4 ElectroBeta cells, respectively. 2 weeks after transfection, populations producing different levels of mCherry fluorescence were isolated by FACS-mediated cell sorting. Monoclonal cell lines were harvested by random picking and cultivation of 25 Electro-Foldon-derived single cell clones.

Microencapsulation of mammalian cells

Intraperitoneal implants were produced by encapsulating wildtype or transgenic 1.1E7 monoclone cells into alginate-poly-(L-lysine)-alginate beads (about 1000 cells per capsule) using B-395 Pro Encapsulator (BÜCHI Labortechnik AG; Flawil, Switzerland) set to the following parameters: a 200 μm nozzle with a vibration frequency of 1300 Hz, using 20 mL syringe. T1DM mice were intraperitoneally injected with 1 mL of FBS-free DMEM containing 1×10^7 cells.

Native and SDS-polyacrylamide gel electrophoresis (PAGE) experiments

48 h after transfection, cells were lysed with PMSF-containing lysis buffer on ice for 15 min, followed by centrifugation at 12,000 rpm and 4 °C for 10 min. The supernatant was collected as protein sample. After treatment with 5x Native Gel Sample Loading Buffer (for native PAGE) or 5xSDS-PAGE Loading Buffer (followed by denaturation at 94 °C for 5 min), same amounts of native or denatured protein samples were resolved on BeyoGel™ Plus Precast PAGE Gel for Tris-Gly System and electroblotted onto Polyvinylidene fluoride (PVDF) Western blotting membranes. Membranes were incubated in BeyoECL Moon detection reagent and visualized using the Amersham Imager 680 (GE Healthcare; Uppsala, Sweden) after application of Mouse anti-FLAG OctA-Probe Antibody (H-5) and secondary HRP-labeled Goat Anti-Mouse IgG (H + L).

Fluorescence imaging

Cells were grown at 37 °C and culture medium was exchanged into serum-free RPMI medium containing or not containing Grazoprevir. Fluorescence microscopy of GCaMP6f signals was performed with a Nikon ECLIPSE Ts2-FL fluorescence microscope equipped with a C-LEDFL470 LED unit as excitation source (488 nm) and a single bandpass filter BA 534/55 for collection of emitted light. Videos were recorded right after stimulation. Elliptical ROI were stacked using ImageJ program every 0.5 s, with the achieved maximum $\Delta F/F_0$ (fluorescence changes versus fluorescence values at time-zero) plotted against recording time.

Flow cytometry

StimExoINS cells were treated with 0.5 μM Grazoprevir or 40 mM KCl for 1 h, with non-treated cells (blank) and vehicle treatment (0.1% DMSO) used as controls. After 24 h, all treatment groups were harvested through trypsinization and centrifugation, washed twice with ice-cold PBS, and stained with the Annexin V-FITC/PI Apoptosis Detection Kit according to the manufacturer's instructions. Cell

populations were then analyzed with a CytoFLEX LX Flow Cytometer (Beckman Coulter, Indianapolis, IN) equipped for green- (488 nm laser, 525/40 emission filter; Annexin V signals) and red fluorescence-detection (561 nm laser, 610/20 emission filter; Propidium Iodide signals). 10,000 cells were recorded per data set and analyzed with FlowJo™ Software (v10; BD Biosciences). The gating strategy involves initial FSC and SSC gates to isolate single, viable cells from the starting population, excluding debris and aggregates.

Cell membrane integrity assay

The integrity of the cell membrane following Grazoprevir stimulation was assessed using Bestbio Cell Membrane Integrity Assay Kits by either fluorescent imaging or absorbance measurement. Before cell seeding, cultivation plates were treated with 0.1 mg/mL poly-D-lysine and the fluorescent dye (BBcellProbe®) was diluted at a ratio of 1:2000 followed by incubation for 2 min. Ethanol served as the positive control of cell membrane damage resulting in BBcellProbe® influx.

RNA sequencing

Total RNA of cells was isolated using the Trizol RNA Extraction method. In brief, 400,000 cells were mixed with 1 ml TRIzol™ Reagent and vortexed until no precipitation was observed. The cell lysate was then mixed with 200 µl chloroform and centrifuged at 12,000 g and 4 °C for 15 min before the aqueous phase was collected and mixed with 500 µl isopropanol to precipitate the RNA (through incubation at −20 °C for 30 min). The RNA pellet was harvested by centrifugation at 4 °C and 15,000 g for 30 min and washed with 70% EtOH. The RNA pellet was air dried and resuspended in 50 µl RNase-free ddH_2O. The libraries were sequenced by Genewiz Biotechnology Co., Ltd. (Suzhou, China) for RNA-seq analysis.

Analytical assays

SEAP assay. Expression levels of human placental secreted alkaline phosphatase (SEAP) in culture supernatants were quantified according to a p-nitrophenylphosphate-based light absorbance time course. In brief, 80 µL of heat-inactivated supernatants (30 min at 65 °C) were transferred to a 96-well plate containing 100 µL of 2x SEAP assay buffer per well. Immediately after addition of 20 mM pNPP per well, Time-dependent increase of light absorbance at 405 nm was followed over 30 min using a Thermo Scientific™ Varioskan™ LUX multimode microplate reader.

NanoLuc assay. NanoLuc levels were profiled using the Nano-Glo® Luciferase Assay System by adding 7.5 µL of a 50:1 (v/v) buffer-substrate mix to 7.5 µL sample per well in a black 384 well plate, followed by luminescence recording on a Thermo Scientific™ Varioskan™ LUX multimode microplate reader.

Insulin ELISA. Insulin levels in culture supernatants and mouse serum were quantified with a Mercodia Mouse Insulin ELISA kit.

Beta-endorphin ELISA. Beta-endorphin levels in cell culture were quantified with a Mouse beta-endorphin ELISA kit (detection range: 0–100 pg/mL).

Animal experiments

Animal ethics. All experiments involving animals were performed according to the directive of the Institutional Animal Care and Use Committee of Westlake University, approved animal protocol number **AP#23-052-XMQ**. 8-week healthy wildtype *C57/BL6J* male mice were purchased from Vital River Laboratories (Beijing, China) and housed in Laboratory Animal Resources Center of Westlake University. Mice were kept at a constant temperature and humidity and exposed to 12 h cycles of alternating light and dark, with ad libitum access to standard rodent food and water. After experiments were completed, mice were euthanized by CO_2 inhalation.

Type-1 diabetes model. The type-1 diabetes mellitus mouse model was generated with 8-week healthy wildtype *C57/BL6J* male mice as described previously[64]. In brief, mice were fasted for 16 h and received intraperitoneal injections of 50 mg/kg streptozotocin (STZ) in freshly prepared citrate buffer within 5 min in dark on five consecutive days. 3 weeks after STZ administration, glycaemia of mice was measured with a commercial Sinocare glucometer. After 4 h fasting, wild-type and T1DM mice receiving cell implants were administrated with saline or 1 mg/kg grazoprevir dissolved in saline.

Blood sampling. Blood was collected from retroorbital plexus of mice by placing whole blood samples at room temperature for 1 h followed by centrifugation for 10 min at 1500 g and 4 °C to obtain serum

Data analysis

For transcriptional experiments, data were shown as mean ± SD, $n = 3$ independent experiments (Fig. 1D, E; Fig. 2B; Fig. 3A, B; Figure S1; Figure S8A, B). For GCaMP detection experiments, data were shown as mean ± SEM, $n = 10$ cells (Fig. 3C, E; Fig. 4B, D; Fig. 6D). For exocytosis experiments, data were shown as mean ± SEM, $n = 3$ independent experiments (Fig. 4C, E; Fig. 5B–D; Fig. 6B–F; Figures S5–S7). For membrane integrity analysis experiment, data were shown as mean ± SD, $n = 4$ independent experiments (Figure S2B). For animal experiments, data were shown as mean ± SEM, n = 4 mice (Fig. 6G, H; Figure S9). Two-tailed unpaired Student t-tests were used to evaluate the statistical significance of differences between two groups. *P*-values more than 0.05 were considered statistically not significant. $^{*}p < 0.05$, $^{**}p < 0.01$, $^{***}p < 0.001$, $^{****}p < 0.0001$. All analyses were performed using GraphPad Prism (v9). Data of RNA sequencing (Figure S3) were processed following the standard data analysis pipeline. Statistical analysis was performed with *Deseq2* (v.1.44.0) package[65]. Significantly changed genes were identified by $|\log_2 FC| > 0.3$, $P < 0.05$ (*P*-value by Wald test). Unsupervised clustering and heatmap visualization were performed with *pheatmap* (V1.0.12). GO and pathway grouping and enrichment analysis were performed by *clusterProfiler* (V4.12.0)[66].

Reporting summary

Further information on research design is available in the Nature Portfolio Reporting Summary linked to this article.

Data availability

All data are available within the article and its Supplementary Information. Raw data generated in this study are provided in the Source Data file. RNA-seq data has been deposited to SRA (Accession no. PRJNA1226287). Source data are provided with this paper.

References

1. Bashor, C. J., Hilton, I. B., Bandukwala, H., Smith, D. M. & Veiseh, O. Engineering the next generation of cell-based therapeutics. *Nat. Rev. Drug Discov.* **21**, 655–675 (2022).
2. Lee, S., Khalil, A. S. & Wong, W. W. Recent progress of gene circuit designs in immune cell therapies. *Cell Syst.* **13**, 864–873 (2022).
3. Teixeira, A. P. & Fussenegger, M. Engineering mammalian cells for disease diagnosis and treatment. *Curr. Opin. Biotechnol.* **55**, 87–94 (2019).
4. Rössger, K., Charpin-El-Hamri, G. & Fussenegger, M. A closed-loop synthetic gene circuit for the treatment of diet-induced obesity in mice. *Nat. Commun.* **4**, 2825 (2013).
5. Bai, P. et al. A synthetic biology-based device prevents liver injury in mice. *J. Hepatol.* **65**, 84–94 (2016).
6. Ye, H. et al. Self-adjusting synthetic gene circuit for correcting insulin resistance. *Nat. Biomed. Eng.* **1**, 0005 (2017).

7. Ye, H., Daoud-El Baba, M., Peng, R.-W. & Fussenegger, M. A synthetic optogenetic transcription device enhances blood-glucose homeostasis in mice. *Science* **332**, 1565–1568 (2011).
8. Turtle, C. J. et al. CD19 CAR-T cells of defined CD4+:CD8+ composition in adult B cell ALL patients. *J. Clin. Invest.* **126**, 2123–2138 (2016).
9. Li, H.-S. et al. Multidimensional control of therapeutic human cell function with synthetic gene circuits. *Science* **378**, 1227–1234 (2022).
10. Zhu, I. et al. Modular Design of Synthetic Receptors for Programmed Gene Regulation in Cell Therapies. *Cell* **185**, 1431–1443.e16 (2022).
11. Chen, C. et al. Genetic-code-expanded cell-based therapy for treating diabetes in mice. *Nat. Chem. Biol.* **18**, 47–55 (2022).
12. Shao, J. et al. Engineered poly(A)-surrogates for translational regulation and therapeutic biocomputation in mammalian cells. *Cell Res* **34**, 31–46 (2024).
13. Mahameed, M., Xue, S., Stefanov, B., Hamri, G. C. & Fussenegger, M. Engineering a Rapid Insulin Release System Controlled By Oral Drug Administration. *Adv. Sci.* **9**, 2105619 (2022).
14. Praznik, A. et al. Regulation of protein secretion through chemical regulation of endoplasmic reticulum retention signal cleavage. *Nat. Commun.* **13**, 1323 (2022).
15. Mansouri, M., Ray, P. G., Franko, N., Xue, S. & Fussenegger, M. Design of programmable post-translational switch control platform for on-demand protein secretion in mammalian cells. *Nucleic Acids Res.* **51**, e1 (2023).
16. Heidelberger, R., Heinemann, C., Neher, E. & Matthews, G. Calcium dependence of the rate of exocytosis in a synaptic terminal. *Nature* **371**, 513–515 (1994).
17. Dolenšek, J., Skelin, M. & Rupnik, M. S. Calcium dependencies of regulated exocytosis in different endocrine cells. *Physiol. Res.* **60**, S29–38 (2011).
18. Stefanov, B.-A., Mansouri, M., Charpin-El Hamri, G. & Fussenegger, M. Sunlight-Controllable Biopharmaceutical Production for Remote Emergency Supply of Directly Injectable Therapeutic Proteins. *Small* **18**, 2202566 (2022).
19. Krawczyk, K. et al. Electrogenetic cellular insulin release for real-time glycemic control in type 1 diabetic mice. *Science* **368**, 993–1001 (2020).
20. Mansouri, M. et al. Smartphone-Flashlight-Mediated Remote Control of Rapid Insulin Secretion Restores Glucose Homeostasis in Experimental Type-1 Diabetes. *Small* **17**, 2101939 (2021).
21. Soboloff, J., Rothberg, B. S., Madesh, M. & Gill, D. L. STIM proteins: dynamic calcium signal transducers. *Nat. Rev. Mol. Cell Biol.* **13**, 549–565 (2012).
22. Bakowski, D., Murray, F. & Parekh, A. B. Store-Operated Ca2+ Channels: Mechanism, Function, Pharmacology, and Therapeutic Targets. *Annu. Rev. Pharmacol. Toxicol.* **61**, 629–654 (2021).
23. Parekh, A. B. & Putney, J. W. Store-Operated Calcium Channels. *Physiological Rev.* **85**, 757–810 (2005).
24. Shrestha, N. et al. Mapping interactions between the CRAC activation domain and CC1 regulating the activity of the ER Ca2+ sensor STIM1. *J. Biol. Chem.* **298**, 102157 (2022).
25. Fahrner, M. et al. A coiled-coil clamp controls both conformation and clustering of stromal interaction molecule 1 (STIM1). *J. Biol. Chem.* **289**, 33231–33244 (2014).
26. Park, H. et al. Optogenetic protein clustering through fluorescent protein tagging and extension of CRY2. *Nat. Commun.* **8**, 30 (2017).
27. O'Shea, E. K., Klemm, J. D., Kim, P. S. & Alber, T. X-ray structure of the GCN4 leucine zipper, a two-stranded, parallel coiled coil. *Science* **254**, 539–544 (1991).
28. Ohshima, T., Yamamoto, H., Sakamaki, Y., Saito, C. & Mizushima, N. NCOA4 drives ferritin phase separation to facilitate macroferritinophagy and microferritinophagy. *J. Cell Biol.* **221**, e202203102 (2022).
29. Kyung, T. et al. Optogenetic control of endogenous Ca2+ channels in vivo. *Nat. Biotechnol.* **33**, 1092–1096 (2015).
30. Barak, Y. et al. Matching fusion protein systems for affinity analysis of two interacting families of proteins: the cohesin-dockerin interaction. *J. Mol. Recognit.* **18**, 491–501 (2005).
31. Chemically induced proximity in biology and medicine. https://www.science.org/doi/10.1126/science.aao5902, https://doi.org/10.1126/science.aao5902.
32. Klewer, L. & Wu, Y.-W. Light-Induced Dimerization Approaches to Control Cellular Processes. *Chem. – A Eur. J.* **25**, 12452–12463 (2019).
33. Van Duyne, G. D., Standaert, R. F., Karplus, P. A., Schreiber, S. L. & Clardy, J. Atomic Structures of the Human Immunophilin FKBP-12 Complexes with FK506 and Rapamycin. *J. Mol. Biol.* **229**, 105–124 (1993).
34. Chin, S. E. et al. A simeprevir-inducible molecular switch for the control of cell and gene therapies. *Nat. Commun.* **14**, 7753 (2023).
35. Foight, G. W. et al. Multi-input chemical control of protein dimerization for programming graded cellular responses. *Nat. Biotechnol.* **37**, 1209–1216 (2019).
36. Xie, M. & Fussenegger, M. Mammalian designer cells: Engineering principles and biomedical applications. *Biotechnol. J.* **10**, 10051018 (2015).
37. Pang, Z. P. & Südhof, T. C. Cell biology of Ca2+-triggered exocytosis. *Curr. Opin. Cell Biol.* **22**, 496–505 (2010).
38. Burgoyne, R. D. & Morgan, A. Secretory Granule Exocytosis. *Physiological Rev.* **83**, 581–632 (2003).
39. Zouboulis, C. C. Human Skin: An Independent Peripheral Endocrine Organ. *Horm. Res. Paediatr.* **54**, 230–242 (2000).
40. Fell, G. L., Robinson, K. C., Mao, J., Woolf, C. J. & Fisher, D. E. Skin β-endorphin mediates addiction to ultraviolet light. *Cell* **157**, 1527–1534 (2014).
41. Burns, S. M. et al. High-Throughput Luminescent Reporter of Insulin Secretion for Discovering Regulators of Pancreatic Beta-Cell Function. *Cell Metab.* **21**, 126–137 (2015).
42. Lim, D. et al. Engineering designer beta cells with a CRISPR-Cas9 conjugation platform. *Nat. Commun.* **11**, 4043 (2020).
43. Choi, J. et al. Light-stimulated insulin secretion from pancreatic islet-like organoids derived from human pluripotent stem cells. *Mol. Ther.* **31**, 1480–1495 (2023).
44. Katsarou, A. et al. Type 1 diabetes mellitus. *Nat. Rev. Dis. Prim.* **3**, 17016 (2017).
45. Geurts, A. M. et al. Gene transfer into genomes of human cells by the sleeping beauty transposon system. *Mol. Ther.* **8**, 108–117 (2003).
46. Krishnan, R., Alexander, M., Robles, L., Foster, C. E. 3rd & Lakey, J. R. T. Islet and Stem Cell Encapsulation for Clinical Transplantation. *Rev. Diabet. Stud.: RDS* **11**, 84 (2014).
47. McNerney, M. P., Doiron, K. E., Ng, T. L., Chang, T. Z. & Silver, P. A. Theranostic cells: emerging clinical applications of synthetic biology. *Nat. Rev. Genet* **22**, 730–746 (2021).
48. Lim, W. A. The emerging era of cell engineering: Harnessing the modularity of cells to program complex biological function. *Science* **378**, 848–852 (2022).
49. Xie, M. et al. β-cell-mimetic designer cells provide closed-loop glycemic control. *Science* **354**, 1296–1301 (2016).
50. Mansouri, M., Strittmatter, T. & Fussenegger, M. Light-Controlled Mammalian Cells and Their Therapeutic Applications in Synthetic Biology. *Adv. Sci. (Weinh.)* **6**, 1800952 (2019).
51. Wang, H., Ye, H., Xie, M., Daoud El-Baba, M. & Fussenegger, M. Cosmetics-triggered percutaneous remote control of transgene expression in mice. *Nucleic Acids Res.* **43**, e91 (2015).

52. Shao, J. et al. Smartphone-controlled optogenetically engineered cells enable semiautomatic glucose homeostasis in diabetic mice. *Sci. Transl. Med.* **9**, eaal2298 (2017).
53. Stanton, B. Z., Chory, E. J. & Crabtree, G. R. Chemically induced proximity in biology and medicine. *Science* **359**, eaao5902 (2018).
54. Kwak, H. et al. Astrocytes Control Sensory Acuity via Tonic Inhibition in the Thalamus. *Neuron* **108**, 691–706.e10 (2020).
55. Kim, S. et al. Non-invasive optical control of endogenous Ca2+ channels in awake mice. *Nat. Commun.* **11**, 210 (2020).
56. Bohineust, A., Garcia, Z., Corre, B., Lemaître, F. & Bousso, P. Optogenetic manipulation of calcium signals in single T cells in vivo. *Nat. Commun.* **11**, 1143 (2020).
57. Wang, X. et al. A programmable protease-based protein secretion platform for therapeutic applications. *Nat. Chem. Biol.* 1–11. https://doi.org/10.1038/s41589-023-01433-z (2023).
58. Mahameed, M., Wang, P., Xue, S. & Fussenegger, M. Engineering receptors in the secretory pathway for orthogonal signalling control. *Nat. Commun.* **13**, 7350 (2022).
59. Jazbec, V., Jerala, R. & Benčina, M. Proteolytically Activated CRAC Effectors through Designed Intramolecular Inhibition. *ACS Synth. Biol.* **11**, 2756–2765 (2022).
60. Monteys, A. M. et al. Regulated control of gene therapies by drug-induced splicing. *Nature* **596**, 291–295 (2021).
61. Calafiore, R. et al. Standard Technical Procedures for Microencapsulation of Human Islets for Graft into Non-immunosuppressed Patients With Type 1 Diabetes Mellitus. *Transplant. Proc.* **38**, 1156–1157 (2006).
62. Li, P., Müller, M., Chang, M. W., Frettlöh, M. & Schönherr, H. Encapsulation of Autoinducer Sensing Reporter Bacteria in Reinforced Alginate-Based Microbeads. *ACS Appl Mater. Interfaces* **9**, 22321–22331 (2017).
63. Pagliuca, F. W. et al. Generation of Functional Human Pancreatic β Cells In Vitro. *Cell* **159**, 428–439 (2014).
64. Furman, B. L. Streptozotocin-Induced Diabetic Models in Mice and Rats. *Curr. Protoc.* **1**, e78 (2021).
65. Love, M. I., Huber, W. & Anders, S. Moderated estimation of fold change and dispersion for RNA-seq data with DESeq2. *Genome Biol.* **15**, 550 (2014).
66. Wu, T. et al. clusterProfiler 4.0: A universal enrichment tool for interpreting omics data. *Innov. (Camb)* **2**, 100141 (2021).

Acknowledgements

We thank Kiryl D. Piatkevich, Yukai Wang and Shichao Li for generous advice and members of Westlake University Biomedical Research Core Facilities (BRCF) and Laboratory Animal Resources Center (LARC) for technical support. Work in the laboratory of M.X. is supported by the National Natural Science Foundation of China (Project no. 32071429), the Ministry of Science and Technology (MOST Project 2020YFA0909200), the HRHI program 202209009 of Westlake Laboratory of Life Sciences and Biomedicine, Tencent Foundation, Westlake Education Foundation and Westlake University Center of Synthetic Biology and Integrated Bioengineering.

Author contributions

Y.S. and M.X. conceived the project and designed the experiments. Y.S., Y.L., J.J., M.H., Y.F., and S.X. performed the experimental work. Y.S., Y.L. M.H., J.J., X.Q., and M.X. analyzed the results. Y.S. and M.X. wrote the manuscript. M.X. received funding and supervised the project. All authors read, corrected and approved the manuscript.

Competing interests

Yaqing Si, Yukai Wang, Yuxuan Fan and Mingqi Xie are inventors on a PCT Patent application PCT/CN2025/077547 (submitted with priority date: Feb 17 2025), "Methods and Systems for Regulating Protein Oligomerization", submitted by Westlake University (applicant) containing all figures, methods and sequences listed in this paper.

Additional information

Supplementary information The online version contains supplementary material available at https://doi.org/10.1038/s41467-025-58184-9.

Correspondence and requests for materials should be addressed to Mingqi Xie.

Peer review information *Nature Communications* thanks Tao Liu, and the other anonymous reviewer(s) for their contribution to the peer review of this work. A peer review file is available.